

Typeset by  $\text{\textit{AMS-TEX}}$

exhibit extremely complex dynamics [3,4] and can, therefore, be used as tools to model a real-life population.

There have been two major approaches towards modelling real-life population growth, namely, continuous and discrete. In the case of the former, one can use differential equations to model the population effectively taking an infinitesimal time-step between generations. On the other hand in the latter case, it is worthwhile to use a simple deterministic model, which determines the population at the next generation in terms of that at the present time-point. The second method is much simpler to use as it involves application of an iterative algorithm to generate the successive population sizes. However, surprisingly enough discrete models are found to show extremely complex dynamics, which includes period-doubling bifurcations and chaos.

In the present study of single-species and host-parasite systems, use has been made of a discrete model, viz., the Hassell model [5]. The stability analysis that we carried out analytically has also been presented. The period-doubling and chaos exhibited by the discrete models can be attributed to the fact that ecological communities show several unstable dynamical states, which can change with very small perturbation. In our study, we have first analyzed the dynamics of a population when it is acting in isolation from any external effects. The only limiting factor in this case, therefore, is related to the density of the population, which tends to inhibit the growth above a certain threshold called the *carrying capacity*. Such effects, known as the density-dependent effects, are incorporated in the model of the population when it is considered to exist in the absence of any external influence. In addition, we have also examined the effect of migration as an external force and studied the change in the system dynamics. We have then considered a coupled system like a host-parasite system where the growth of the host and that of the parasite are governed by the Hassell law.

## 2. THE MODEL

In formulating our model, we make use of the growth function [5] given by

$$X_{t+1} = \frac{RX_t}{(1 + X_t)^b}, \quad (1)$$

in which  $X(t)$  stands for the population size at time  $t$ ,  $R$  is the intrinsic growth rate of the population, and  $b$  incorporates density-dependent effects such as intra-specific competition. The above equation gives us the population size at time  $t+1$  in terms of the population at time  $t$ . The return maps of the model for different values of the parameters  $R$  and  $b$  are shown in Figures 1 and 2.

The return maps indicate that the height of the peak of the population growth increases with increasing  $R$  and decreasing  $b$ . The peak becomes sharper for larger  $R$  and also for increasing  $b$ . This is because increasing  $R$  denotes a population that grows fast owing to which we get a higher peak, while increasing  $b$  indicates a tighter bound on the population size due to intra-specific competition as a result of which the peak becomes smaller and sharper.

The above situation holds true for a population, which is not affected by any environmental factors. We introduce a constant diffusive force  $L$  into the model as a control of the population, so that

$$X_{t+1} = f(X_t) = \frac{RX_t}{(1 + X_t)^b} + L. \quad (2)$$

In the case of a population, a diffusive force stands for migration which when positive is called *immigration* and when negative is termed *emigration*. The return map of the model with positive and negative migration is shown in Figure 3. The continuous line indicates the return map for positive migration, while the dotted line represents negative migration. As expected, the map shows a lateral increase in the values with no change in its form as compared to the plot without migration. The identity line represents the points where the population is unchanged at two

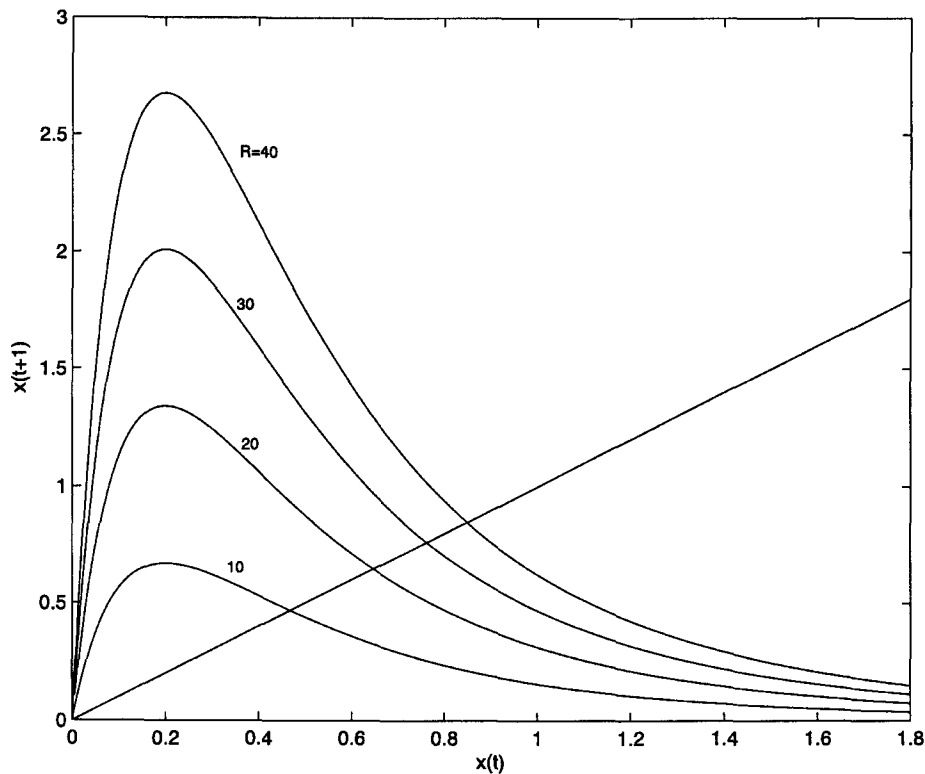


Figure 1. Return map of the Hassell growth function for different values of the parameter  $R$  when  $b = 6$ .

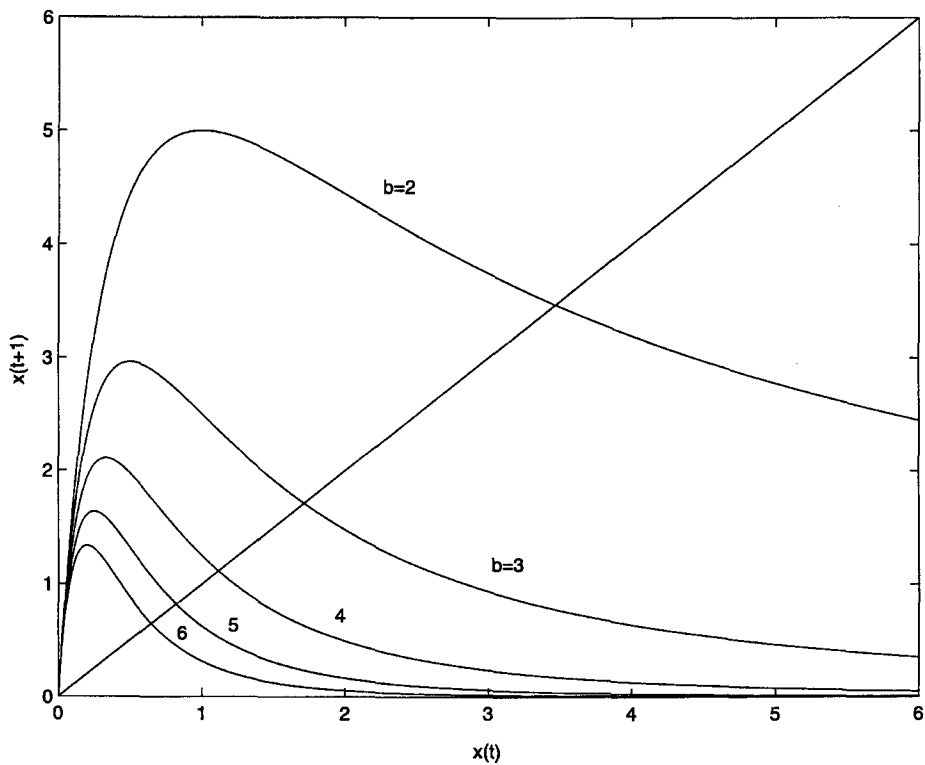


Figure 2. Return map of the Hassell growth function for different values of  $b$  when  $R = 20$ .

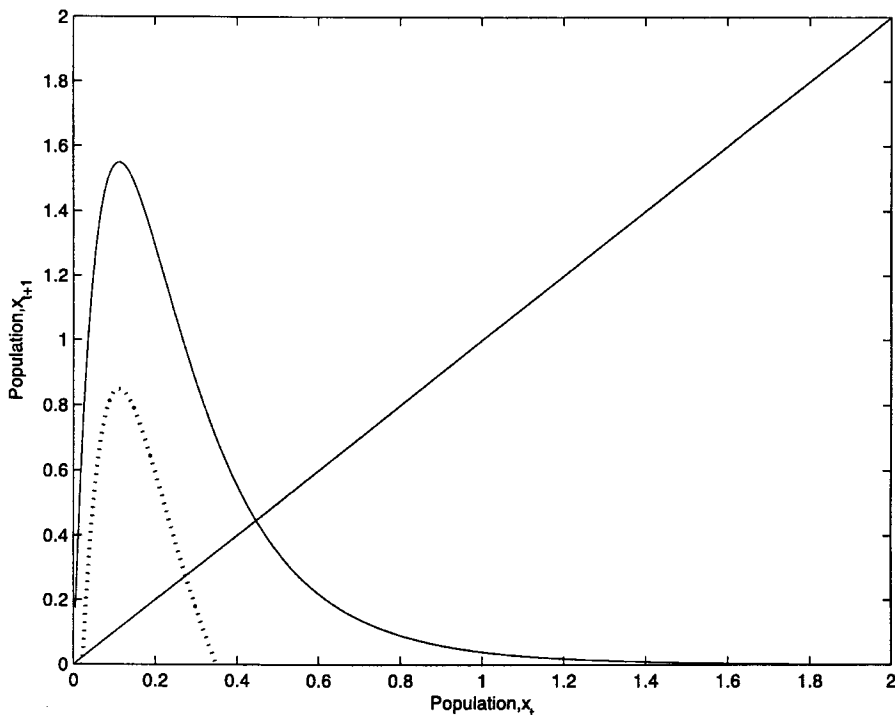


Figure 3. Return map of the model with positive (continuous line) and negative (dotted line) migration, when  $b = 10$ ,  $R = 40$ .

successive time-points. Hence, the intersection of the identity line with the return maps gives us the steady-states of the system.

The curve representing the population sizes with positive migration cuts the identity line at only one point, which is the stable steady state, while the curve for negative migration cuts the identity line at two points giving rise to two steady states in the system, one of which (the one closer to the origin) is unstable, i.e., if the population happens to reach a value close to this region, it goes to extinction for even a small ecological change. Hence, such a situation can be highly sensitive for the population in question.

### 3. ANALYSIS

For a fixed point,

$$X_{t+1} = X_t.$$

Using (1), for determining a fixed point  $x_p$ , we can write

$$\frac{Rx_p}{(1+x_p)^b} = x_p.$$

The two solutions are

$$x_p = 0, \left(R^{1/b} - 1\right).$$

The critical point  $x_c$  is one where the birth (due to the intrinsic growth rate) and death processes (due to density-dependent effects) balance each other and the tangent to the growth curve is zero.

Writing

$$g(x) = \frac{Rx}{(1+x)^b},$$

if  $x_c$  is a critical point, we have

$$g'(x_c) = 0,$$

which yields

$$R(1 + x_c) - bRx_c = 0,$$

so that

$$x_c = \frac{1}{(b-1)}.$$

It may be noted that for this value of  $x_c$ ,

$$g''(x_c) = \frac{bR}{(1+x)^{b+2}} [(b-1)x_c - 2] < 0.$$

#### 4. LOCAL STABILITY OF STEADY STATES

We now examine the stability of the steady states at 0 and  $R^{1/b} - 1$ . For the Hassell function given by equation (1), we write

$$x = F(x, R, b) = \frac{Rx}{(1+x)^b}.$$

Then

$$J = \frac{\partial F}{\partial x} = \frac{R[1 + (1-b)x]}{(1+x)^{b+1}}.$$

To test the stability of the steady states, we have to find the values of  $J$ , which serve as the eigenvalues of the one-variable system.

At  $x = 0$ ,

$$\lambda = R > 0,$$

so that the system is unstable.

For  $x = R^{1/b} - 1$ ,

$$\lambda = R^{-1/b} \left[ 1 + (1-b) \left( R^{1/b} - 1 \right) \right].$$

For saddle-node bifurcation, one must have

$$|J| = \left| \frac{\partial F}{\partial x} \right| = 1.$$

In order that the steady state is stable,

$$\frac{\partial F}{\partial x} = -1,$$

that is,

$$R^{-1/b} \left[ 1 + (1-b) \left( R^{1/b} - 1 \right) \right] = -1,$$

which yields

$$R = \left( \frac{b}{b-2} \right)^b.$$

## 5. HOST-PARASITE SYSTEM

Having looked at the dynamics of a single-species population under the effects of intra-specific competition and a constant external perturbation, let us now turn to a two-species interacting system in which we will examine the effect of inter-specific competition. Traditionally, there are two different systems that are studied in this context, a host-parasite system and a predator-prey system.

For the host-parasite system, the classical host-parasite model is the Nicholson-Bailey model, which is based on the following assumptions (that can be justified from a purely biological point-of-view).

- (1) Parasites in the next generation are due to the hosts infected in the present generation.
- (2) Hosts that are not infected give rise to their own progeny.
- (3) The fraction of the host that is infected depends on the rate of encounter of the two species; in general, from the law of mass action this fraction tends to depend upon the density of one or both species.

In the sequel, we shall use the following notations:

$H_t$ : density of host species in generation  $t$ ,

$P_t$ : density of parasite species in generation  $t$ ,

$f(H_t, P_t)$ : fraction of host not infected,

$\mu$ : host reproductive rate,

$c$ : average number of viable eggs laid by a parasite on a single host (fecundity).

Then by virtue of the above three assumptions, we get

$H_{t+1}$  = (number of hosts in the previous generation)  $\cdot$  (fraction of host not infected)  $\cdot$  (reproductive rate of the host),

$P_{t+1}$  = (number of hosts infected in the previous generation)  $\cdot$  (fecundity of parasites).

Therefore, the equations turn out to be

$$H_{t+1} = \mu H_t f(H_t, P_t), \quad (3)$$

$$P_{t+1} = c H_t [1 - f(H_t, P_t)]. \quad (4)$$

The Nicholson-Bailey model was developed by using two more assumptions about the number of encounters and the rate of infection of the host, viz.,

- (i) following the law of mass action, the number of encounters  $H_e$  of the hosts by parasites is proportional to the product of their densities, so that

$$H_e = \beta H_t P_t,$$

$\beta$  being a constant known as the searching efficiency of the parasite;

- (ii) only the first encounter between a host and a parasite is significant and the encounter is random.

Because the encounter is assumed to be random, one can represent the probability of  $n$  encounters by a distribution, which is based upon the average number of encounters per unit time.

This situation can be described by using the Poisson distribution, with probability mass function given by

$$P(n) = \frac{e^{-\beta p} (\beta p)^n}{n!} \quad (n = 0, 1, 2, 3, \dots),$$

where  $p$  is number of parasites and  $n$  the number of encounters/time.  $\beta p$  is the mean of the distribution; it stands for the average number of encounters per unit time.

Thus,

$$f(H_t, P_t) = P(0) = e^{-\beta P_t}.$$

Here  $n = 0$ , since only the first encounter of the host is assumed to be significant and is considered to be enough for a successful transfer of the parasite egg.

From (3) and (4), we now have

$$H_{t+1} = \mu H_t e^{-\beta P_t}, \quad (5)$$

$$P_{t+1} = c H_t (1 - e^{-\beta P_t}). \quad (6)$$

Using the Hassell growth function for the host and taking the fecundity ( $c$ ) of parasite as 1, the above equations become

$$H_{t+1} = \frac{R H_t}{(1 + H_t)^b} e^{-\beta P_t}, \quad (7)$$

$$P_{t+1} = H_t (1 - e^{-\beta P_t}). \quad (8)$$

If the steady state values of  $H_t$  and  $P_t$  are denoted by  $H^*$  and  $P^*$ ,

$$\begin{aligned} H^* &= \frac{R H^*}{(1 + H^*)^b} e^{-\beta P^*}, \\ \Rightarrow e^{-\beta P^*} &= \frac{(1 + H^*)^b}{R}, \end{aligned} \quad (9)$$

$$P^* = H^* \left( 1 - \frac{(1 + H^*)^b}{R} \right). \quad (10)$$

Putting the value of  $P^*$  from the above equation into equation (9), we get

$$e^{-\beta H^* \{1 - (1 + H^*)^b / R\}} = \frac{(1 + H^*)^b}{R}.$$

This being a transcendental equation cannot be solved analytically.

The steady state or fixed point is said to be stable if a small perturbation applied to the steady state dies out and the system regains the equilibrium dynamics as it evolves. Let us apply small perturbation  $h_n$  and  $p_n$  to steady state at time step  $n$ . Then at step  $(n + 1)$ , the evolution equations are

$$\begin{aligned} H^* + h_{n+1} &= F(H^* + h_n, P^* + p_n), \\ P^* + p_{n+1} &= G(H^* + h_n, P^* + p_n). \end{aligned}$$

For carrying out the linear stability analysis, expanding in Taylor series the above equations may be rewritten as

$$\begin{aligned} h_{n+1} &= a_{11} h_n + a_{12} p_n, \\ p_{n+1} &= a_{21} h_n + a_{22} p_n, \end{aligned}$$

with

$$a_{11} = \frac{\partial F}{\partial H}, \quad a_{12} = \frac{\partial F}{\partial P}, \quad a_{21} = \frac{\partial G}{\partial H}, \quad \text{and} \quad a_{22} = \frac{\partial G}{\partial P},$$

where all the derivatives are calculated at  $H^*$  and  $P^*$ ,

$$\begin{aligned} F &= \frac{R H}{(1 + H)^b} e^{-\beta P}, \\ G &= H (1 - e^{-\beta P}). \end{aligned}$$

Using (9) and (10), we have further

$$\begin{aligned} a_{11} &= \frac{1 - (b-1)H^*}{1 + H^*}, & a_{21} &= 1 - \frac{(1 + H^*)^b}{R}, \\ a_{12} &= -\beta H^*, & a_{22} &= \beta H^* \left\{ \frac{(1 + H^*)^b}{R} \right\}. \end{aligned}$$

Considering the matrix

$$A = \begin{pmatrix} a_{11} & a_{12} \\ a_{21} & a_{22} \end{pmatrix},$$

the characteristic equation is

$$\begin{vmatrix} a_{11} - \lambda & a_{12} \\ a_{21} & a_{22} - \lambda \end{vmatrix} = 0,$$

which may be rewritten in the form

$$\lambda^2 - B\lambda + C = 0, \tag{11}$$

where

$$\begin{aligned} B &= a_{11} + a_{22}, \\ C &= a_{11}a_{22} - a_{12}a_{21}. \end{aligned}$$

For the perturbation to decay and the steady state to be stable, the magnitude of each of the roots of equation (11), say  $\lambda_1$  and  $\lambda_2$ , has to be less than unity. This requires

$$|B| + \sqrt{B^2 - 4C} < 2,$$

which yields

$$|B| < C + 1.$$

Again, since  $|\lambda_1|, |\lambda_2| < 1$ , we have

$$\lambda_1 \lambda_2 < 1,$$

so that

$$C < 1.$$

Now

$$|B| < C + 1 < 2.$$

If we substitute the values of  $B$  and  $C$  into the above equation, we get the condition for bifurcation in the form

$$\left| \frac{1 - (b-1)H^*}{1 + H^*} + \beta H^* \frac{(1 + H^*)^b}{R} \right| < 1 + \beta H^* \left\{ 1 - \frac{bH^*(1 + H^*)^{b-1}}{R} \right\}, \tag{12}$$

$$1 + \beta H^* \left\{ 1 - \frac{bH^*(1 + H^*)^{b-1}}{R} \right\} < 2. \tag{13}$$

If both equations (12) and (13) are satisfied, the steady state will be stable.



## 5. NUMERICAL RESULTS AND DISCUSSION

Let us now undertake the numerical simulations of the single-species Hassell model, for the case when there is migration, and also when migration is absent. In the sequel, we present the bifurcation diagrams of the model that have been obtained with data from 500 iterations with time-step of 0.1 units, after removing transients. For the case when there is migration, we have used equation (2) iteratively, with  $L$ , the perturbation parameter, being increased in steps of 0.01. In both these cases, the plots have been generated using MATLAB 6.5 on an AMD Athlon 1800 XP computer.

The Hassell model exhibits a variety of dynamical behaviour in respect of the population size, if the controlling parameters  $R$  and  $b$  exceed certain values. The population shows several equilibrium states, and for certain higher values of the parameters there can be infinite number of such possibilities so far as the population size is concerned. This implies that for a particular species, if the intrinsic growth rate is high, in the presence of a high intra-specific competition given by a large value of  $b$ , there is a possibility that it will show sudden spurts or drops in the population for seemingly minute changes in environmental conditions. The dynamics vary from steady (equilibrium) state to chaotic through a hierarchy of bifurcations. This chain of dynamics is exhibited in the bifurcation diagram of  $X$  (Figures 4–7) for different values of  $b$  with  $R$  as the bifurcation parameter.

Figure 4 shows that there is no period-doubling bifurcation for  $b = 2$ , as the population shows a single stable value for  $R$  in the range 0 to 40. However, the dynamical behaviour changes dramatically once we increase the value of  $b$  (cf. Figures 5–7). These figures clearly indicate that for values of  $b > 2$ , the population exhibits period-doubling phenomenon and reveal that the intrinsic growth rate at which the first bifurcation takes place becomes smaller and smaller with increasing  $b$ . This is in accordance with the analytical condition that we have derived in Section 4.

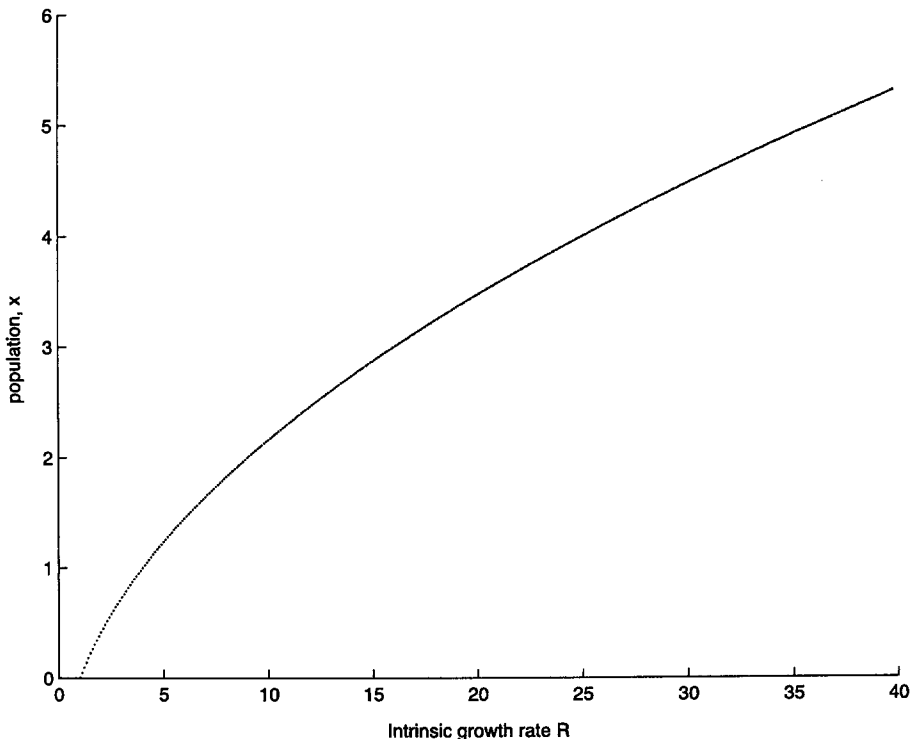


Figure 4. Bifurcation diagram for the Hassell model with intrinsic growth rate  $R$  (bifurcation parameter), when  $b = 2$ .

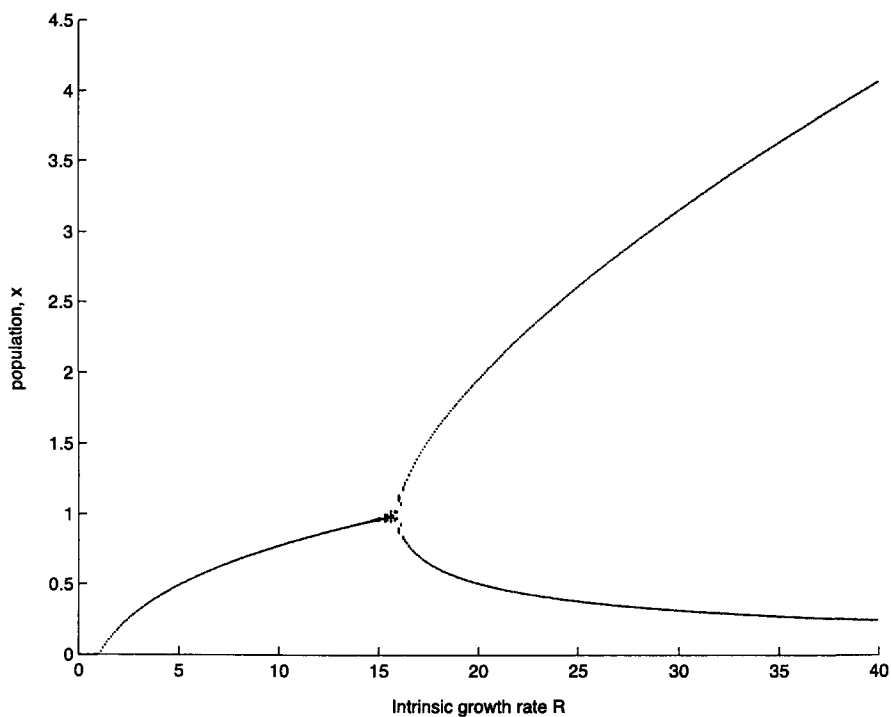


Figure 5. Bifurcation diagram for the Hassell model, when  $b = 4$ .

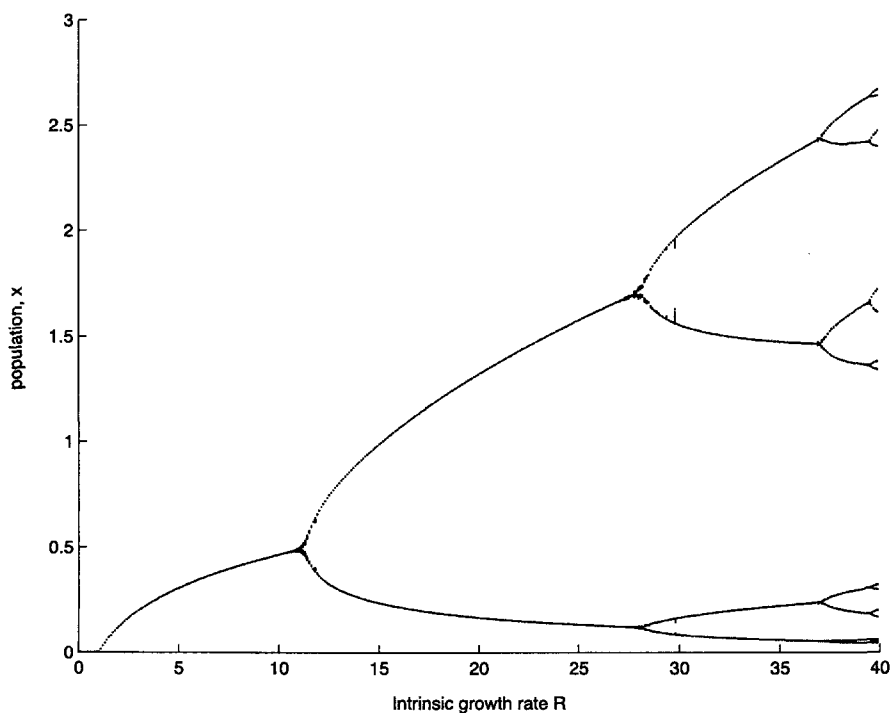


Figure 6. Bifurcation diagram for the Hassell model ( $b = 6$ ).

The parameters represent controls of the system, using which we can control the population sizes. Increasing the parameters effectively makes the bounds on the system tighter and pushes it from stability towards unstable behaviour. This instability manifests itself as a period-doubling

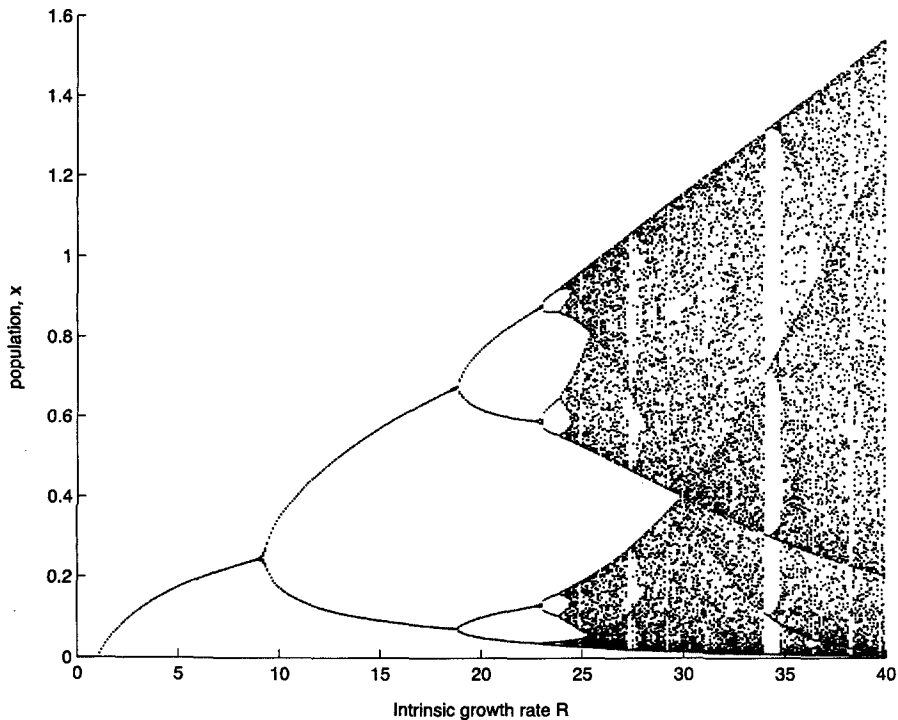


Figure 7. Bifurcation diagram for the Hassell model ( $b = 10$ ).

bifurcation as a result of which the single equilibrium level of the population splits into two and the population starts oscillating between two levels which are quite different in their relative magnitudes. As we keep on increasing the parameters, these levels individually split up more and more frequently, until all order is lost and we find an infinite number of possible equilibrium states visited by the population. At this point, the population behaviour seems to lose any semblance of periodicity.

This appearance of nonperiodic behaviour from equilibrium population levels may be referred to as the “period-doubling route to chaos”, the nonperiodic dynamics being described as *chaotic*. However, even after the system loses all traces of periodicity in its behaviour, out of the chaotic region, there appear sudden *periodic windows*, which are seen to have an odd-periodicity. The chaotic region of the bifurcation diagram (cf. Figure 7) shows periodic windows of a period-3 oscillation. This sudden reappearance of periodic behaviour out of chaos is also observed in several other discrete models, such as the *logistic model*. There have been some studies [5,6] that show the unlikelihood of the appearance of chaos in real-world populations. However, such studies do not dismiss the possibility of a population showing an oscillatory or cyclic nature.

When we introduce migration into the model, we find that the dynamics of the system change quite dramatically. The plots for varying levels of positive or negative perturbation are given in Figures 8–11.

We find that for values of  $R$  giving rise to the stability in the system (Figures 8 and 10), the population size goes to higher values for positive perturbation, while it goes to extinction for negative perturbation. However, the results corresponding to the values of  $R$  which lead to the system instability are most interesting and unusual. With positive perturbation, we find reverse period-doubling bifurcation as the system comes out of unstable dynamics and goes to stable dynamics. For negative perturbation, the population again shows period-reversal to stability, but for some intermediate values, there is indication of escape. However, the positive iterates occur again for higher values of  $L$  after which it goes to stable dynamics.

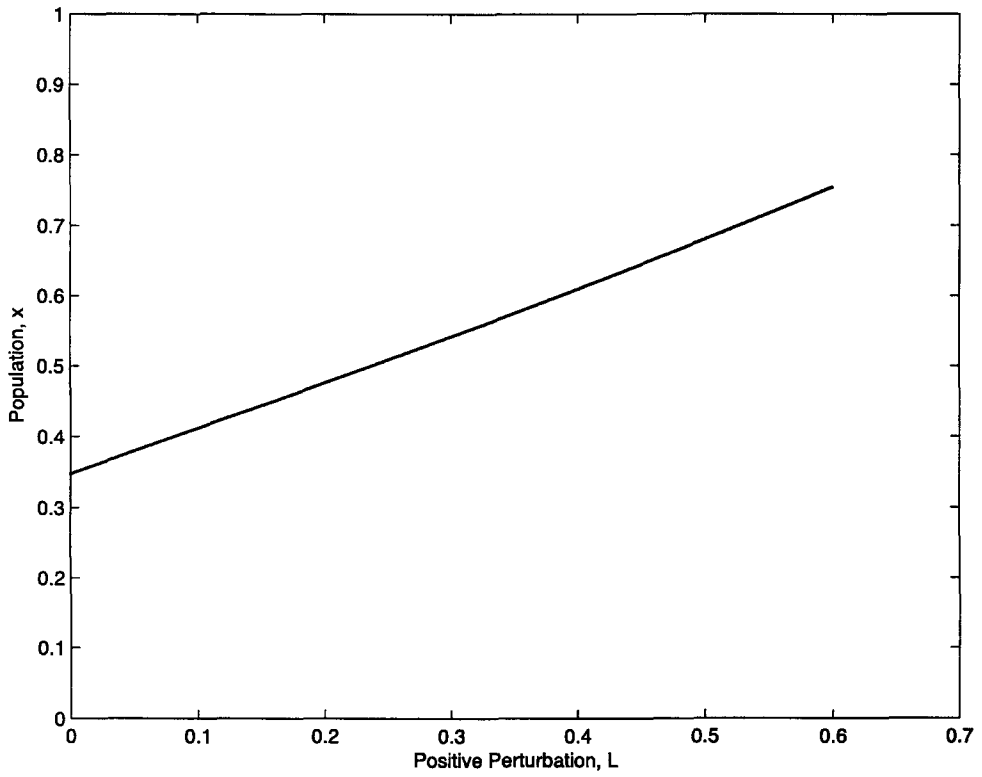


Figure 8. Bifurcation diagram of the Hassell model with migration, when  $b = 6$ ,  $R = 6$ ,  $L > 0$ .

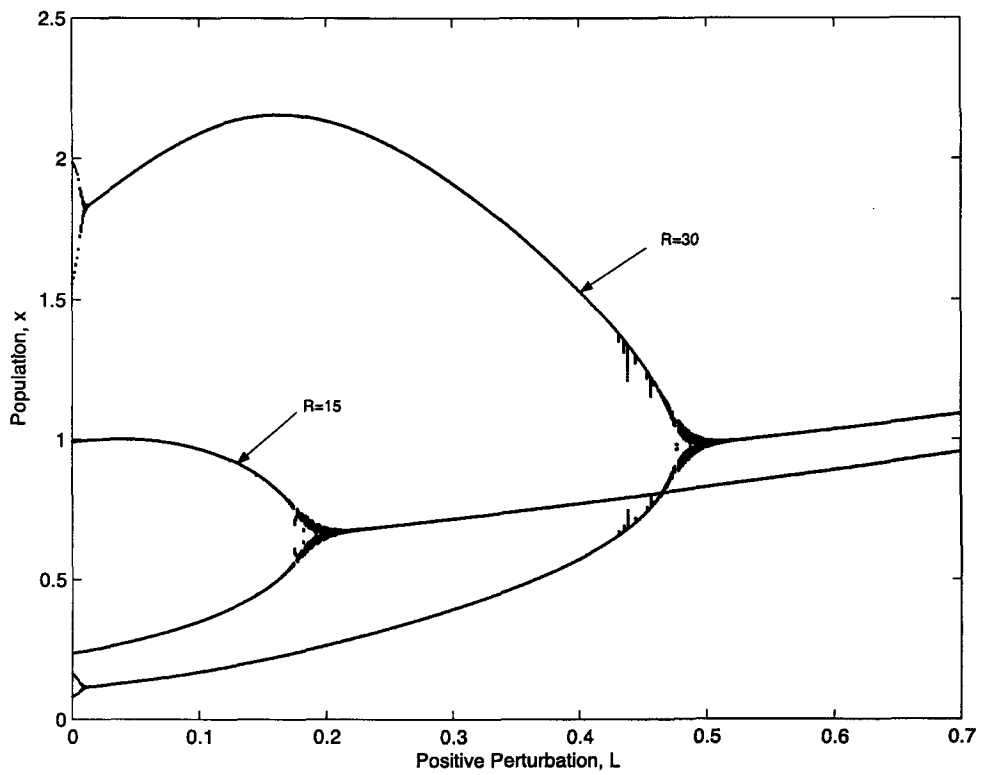


Figure 9. Bifurcation diagram of the Hassell model at  $b = 6$ ,  $L > 0$ .

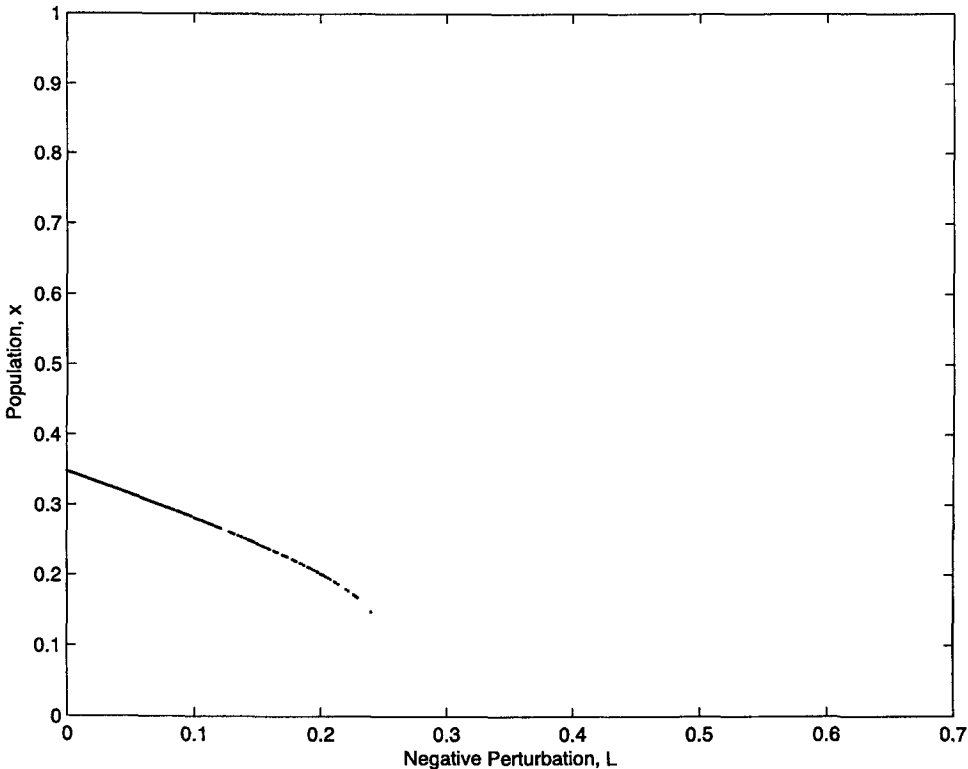


Figure 10. Bifurcation diagram of the Hassell model at  $b = 6$ ,  $R = 6$  (for negative perturbation,  $L$  in equation (2) is replaced by  $-L$ , where  $L > 0$ ).

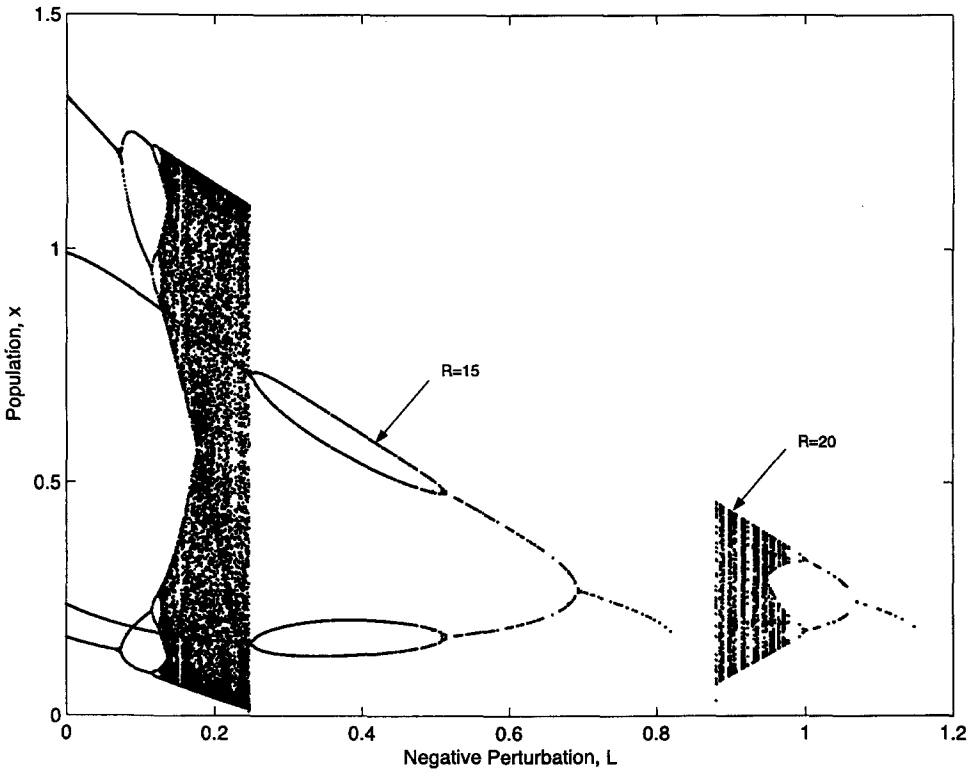


Figure 11. Bifurcation diagram of the Hassell model for negative perturbation at  $b = 6$ .

Such a variation in the behaviour of the system can be interpreted in various ways. We can conclude that for a population that grows rapidly (for higher values of  $R$ ), immigration (positive perturbation) induces stability. This can be understood by considering that the population undergoing large oscillation of period  $2n$  is saved from the possibility of an ecological catastrophe by the steady influx into the system. Hence, migration induces a 'damping' or a 'suppression' of the unstable dynamics.

It is more difficult to visualize the results for negative perturbation or 'emigration'. The chaotic map comes out of chaos and undergoes escape before re-establishing again at higher values of  $L$ . The behaviour is slightly different for different values of  $R$ . In fact, in this case we find that the population shows escape from both stable dynamics ( $R = 15$ ) and also from chaotic oscillatory dynamics ( $R = 20$ ).

This change in the dynamics of the system from chaotic to stable as a result of a constant external perturbation shows that such an effect could be used as an effective control of chaos. This result finds application in the study of certain real-life populations, especially certain pests, and can help understand the patterns in their growth and multiplication.

## 7. CONCLUSIONS

The study of a discrete single-species population with the help of the Hassell growth function yields certain interesting results. The population shows stability for a certain range of parameter values and also exhibits a wide variety of other behaviour when we change the parameters over certain ranges. We have introduced a constant external perturbation in the form of migration and studied its effects on the system dynamics.

We have also examined a two-species interacting system where our treatment is entirely analytical. The system is examined via the techniques of steady-state analysis and local stability analysis of the steady states from which we obtain the bifurcation criterion.

The numerical simulation of the population size shows a succession of period-doubling bifurcations leading up to chaos. The effect of migration on the model depends on the value of the intrinsic growth rate,  $R$ . For values of  $R$  corresponding to the stable system dynamics, the population undergoes a linear change. However, for values of the intrinsic growth rate ( $R$ ) which makes the system dynamics unstable or chaotic, its effect is that of damping as it induces reverse-period doubling bifurcations and results in the appearance of stable dynamics. It may thus be concluded that migration offers a strong control of chaos.

## REFERENCES

1. S.J. Schreiber, Chaos and population disappearances in simple ecological models, *J. Math. Biol.* **42**, 239–260, (2001).
2. A.H. Beeton, Changes in the environment and biota of the Great Lakes, In *Eutrophication: Causes, Consequences, Correctives*, pp. 150–187, National Academy of Sciences, Washington, DC, (1969).
3. R.M. May, Simple mathematical models with very complicated dynamics, *Nature* **269**, 459–475, (1976).
4. R.M. May and G.F. Oster, Bifurcations and dynamics complexity in simple ecological models, *Am. Nat.* **110**, 573–599, (1976).
5. M.P. Hassell, J. Lawton and R.M. May, Pattern of dynamical behaviour in single-species populations, *J. Anim. Ecol.* **45**, 471–486, (1976).
6. L.D. Mueller and F.J. Ayala, Dynamics of single-species population growth: Stability or chaos?, *Ecology* **62** (5), 1148–1154, (1981).